

Supplementary Information

**Synthesis, characterization, magnetic and antibacterial properties of a  
novel iron (III) complex  $(\text{CH}_3)_2\text{NH}_2[\text{Fe}(\text{phen})\text{Cl}_4]$**

Asmae Ben Abdelhadi,<sup>a, b</sup> Sara Rodríguez-Sánchez,<sup>c</sup> Rachid Ouarsal,<sup>a</sup> Mohamed Saadi,<sup>d</sup>  
Lahcen El Ammari,<sup>d</sup> Nicola Morley,<sup>e</sup> Brahim El Bali,<sup>f</sup> Óscar Gómez-Torres,<sup>g</sup> Mohammed  
Lachkar\*,<sup>a</sup> and Abderrazzak Douhal <sup>\*b</sup>

---

*a.* Engineering Laboratory of Organometallic, Molecular Materials, and Environment (LIMOME), Faculty of Sciences, Sidi Mohamed Ben Abdellah University, 30000 Fez, Morocco.

*b.* Departamento de Química Física, Facultad de Ciencias Ambientales y Bioquímica, y INAMOL, Campus Tecnológico de Toledo, Universidad de Castilla-La Mancha (UCLM), Avenida Carlos III, S.N., 45071 Toledo, Spain.

*c.* Departamento de Química Analítica y Tecnología de los Alimentos, Facultad de Ciencias Ambientales y Bioquímica, Universidad de Castilla-La Mancha, Toledo, Spain.

*d.* Laboratoire de Chimie Appliquée des Matériaux, Centre des Sciences des Matériaux, Faculty of Science, Mohammed V University in Rabat, Avenue Ibn Battouta, BP 1014, Rabat, Morocco.

*e.* Department of Materials Science and Engineering, University of Sheffield, Sheffield S1 3JD, United Kingdom.

*f.* Independent Scientist, Marrakech, Morocco.

*g.* Facultad de Ciencias Ambientales y Bioquímica, Universidad de Castilla-La Mancha, Toledo, Spain.

\*Corresponding authors: [mohammed.lachkar@usmba.ac.ma](mailto:mohammed.lachkar@usmba.ac.ma) and [abderrazzak.douhal@uclm.es](mailto:abderrazzak.douhal@uclm.es)

## Index

<b>Experimental Section</b>	Pages 3-
5	
<b>Figure. S1</b> Solubility of the complex $(\text{CH}_3)_2\text{NH}_2[\text{Fe}(\text{phen})\text{Cl}_4]$ in some selected solvents.	Page 5
<b>Table S1:</b> Crystal data and structure refinement parameters of complex <b>1</b> .	Page 6
<b>Table S2:</b> Fractional atomic coordinates and isotropic or equivalent isotropic displacement parameters ( $^{\circ}\text{A}^2$ ).	Page 6-7
<b>Table S3:</b> Bond distances ( $\text{A}^{\circ}$ ) and bond angles ( $^{\circ}$ ) of the complex <b>1</b> .	Pages 8-9
<b>Figure. S2</b> The 2D fingerprint plots of the major contacts of $(\text{CH}_3)_2\text{NH}_2[\text{Fe}(\text{phen})\text{Cl}_4]$ , showing contributions from different contacts: b) $\text{H}\cdots\text{Cl}/\text{Cl}\cdots\text{H}$ , c) $\text{H}\cdots\text{H}$ , d) $\text{H}\cdots\text{C}/\text{C}\cdots\text{H}$ , e) $\text{C}\cdots\text{C}$ and f) $\text{N}\cdots\text{H}/\text{H}\cdots\text{N}$ .	Page 10
<b>Figure. S3</b> Inhibition zone of $(\text{CH}_3)_2\text{NH}_2[\text{Fe}(\text{phen})\text{Cl}_4]$ and the commercially available antibiotic in (mm) at 600 $\mu\text{g}/\text{mL}$ concentration.	Page 11
<b>Figure. S4</b> In vitro antimicrobial activity of $(\text{CH}_3)_2\text{NH}_2[\text{Fe}(\text{phen})\text{Cl}_4]$ against two Gram-negative and two Gram-positive bacteria.	Page 12
<b>References</b>	Page 12

## Experimental Section

### Chemicals

All chemicals and solvents used for the synthesis were of reagent grade quality and were obtained from commercial sources and used as received: FeCl<sub>3</sub>·6H<sub>2</sub>O (reagent grade, ≥ 98%, Sigma-Aldrich), 1,10-phenanthroline hydrochloride monohydrate (≥ 99.5%, Sigma-Aldrich), N, N-dimethylformamide (≥ 99.8%, Sigma-Aldrich), HCl (37%, Sigma-Aldrich).

### Characterization

#### Single and powder crystal X-ray crystallography

A single crystal was carefully selected under a microscope in order to perform its structural analysis by X-ray diffraction technique. X-ray data were collected using a Bruker D8 VENTURE Super DUO diffractometer equipped with monochromated MoK $\alpha$  radiation  $\lambda = 0.71073$  Å at 296 K. The structure of (CH<sub>3</sub>)<sub>2</sub>NH<sub>2</sub>[Fe(phen)Cl<sub>4</sub>] was solved by a dual-space algorithm using the SHELXT program,<sup>1</sup> and then refined with full-matrix least-square methods based on F<sup>2</sup> (SHELXL2014/7) software program.<sup>2</sup> All non-hydrogen atoms were anisotropically refined. The hydrogen atoms were located by Fourier difference synthesis and isotropically refined. The final conventional R(F) = 0.027 and wR(F<sup>2</sup>) = 0.079 for 8526 reflections ( $I > 2\sigma$ ) with weighting scheme,  $w = 1/[\sigma^2(F_o^2) + (0.0399P)^2 + 0.1124P]$ , where  $P = (F_o^2 + 2F_c^2)/3$ . Table S1 shows the crystal data, while table S2 gives the refined atomic position ones. The drawings of the results structure were made using Mercury program. Further details can be found in the deposited CIF at CCDC, with the code CCDC 2281265, using the [www.ccdc.cam.ac.uk](http://www.ccdc.cam.ac.uk) link or from the Cambridge Crystallographic Data Centre. Visualization and exploration of intermolecular contacts of **1** was achieved using the Hirshfeld surface calculated with Crystal Explorer 3.1 software.<sup>3, 4</sup> The molecular Hirshfeld surfaces were generated using standard (high) surface resolutions mapped over a fixed color scale of -0.2271 (red) to 1.3559 Å (blue).

The powder X-ray diffraction (PXRD) pattern was recorded on a PANalytical Xpert-PRO powder diffractometer using Cu-K $\alpha$  radiation (1.5418 Å) with a 2 $\theta$  range of 5-50°. The simulation of the PXRD pattern was carried out by the single-crystal data and Oscale.

### **Elemental analysis, Spectroscopic, thermal gravimetric, magnetization and magnetic susceptibility measurements**

Elemental analysis was conducted at ITQ-CSIC and UPV (Valencia, Spain). To quantify the contents of C, N and H, we used a Carlo Erba 1106 elemental analyzer. While for the Fe one, we used a Varian 715-ES ICP-Optical Emission spectrometer after dissolution of **1** in a HNO<sub>3</sub>/HCl/HF aqueous solution. Infrared spectroscopy measurements were performed using a Vertex 70 (Bruker) Fourier transform infrared spectrometer (FTIR). The IR spectrum was collected between 4000 to 400 cm<sup>-1</sup> using the attenuated total reflectance (ATR) method at a resolution of 4 cm<sup>-1</sup>. UV-Vis spectra were recorded on a JASCO V-670 spectrophotometer equipped with a 60 mm integrating sphere unit (JASCOISN-723). The longitudinal axes of the spectrum were converted using the Kubelka–Munk function from reflectance (%R) to K-M unit  $F(R) = ((1 - R)^2 / (2R))^{-1}$  where R is the diffuse reflectance intensity from the sample. spectrophotometer Lambda 20 in the range 200-800 nm.

Thermogravimetric analysis (TGA) was done on a «The LINSEIS TGA PT1600» at a heating rate of 5°C/min using an open platinum crucible under air flow.

Magnetization and magnetic susceptibility (AC) measurements were carried out in a Quantum Design magnetometer MPMS 5 VSM-SQUID2. instrument, as a function of temperature in the 2-300 K range. The frequency was varied from 10 to 10 kHz in the (AC) susceptibility. (DC) magnetization was done in the field of 100 Oe (Oersted) with the samples in zero field cooled (ZFC) at different temperatures, the measurement was repeated in the same way for the field cooled (FC).

### **Antibacterial activity testing**

The antibacterial activity of the synthesized compound (CH<sub>3</sub>)<sub>2</sub>NH<sub>2</sub>[Fe(phen)Cl<sub>4</sub>] against some potentially pathogenic bacteria was assayed *in vitro*, by using the disc diffusion method.<sup>5</sup> The used pathogenic bacteria (indicator) were from the Colección Española de Cultivos Tipo (CECT). They were comprised both Gram-positive bacteria, *S. aureus* CECT 86 and *L. monocytogenes* CECT 4031, and Gram-negative bacteria belonging to Enterobacteriaceae, *E. coli* CECT 99 and *K. pneumoniae* CECT 143T. All of them were grown in a Tryptic Soy Broth

(TSB), except for *L. monocytogenes* that was in a Brain Heart Infusion (BHI) broth. The incubation temperature was 37°C for all of them.

Cells from overnight cultures in TSB or BHI broth were harvested by centrifugation at 18,500 x g for 5 min at 4°C and suspended in sterile phosphate buffer saline (PBS) at pH = 7.2 to reach the 0.5 McFarland turbidity standard, equivalent to 10<sup>8</sup> colony forming units/mL. These suspensions were smeared on Mueller-Hinton (Pronadisa, Madrid, Spain) agar plates. Blank discs (Oxoid, Hampshire, UK) were used which were spotted with 20 µL of a 5 mg/mL of the complex (CH<sub>3</sub>)<sub>2</sub>NH<sub>2</sub>[Fe(phen)Cl<sub>4</sub>] in Milli-Q water. Ciprofloxacin (5 µg) and chloramphenicol (30 µg) antibiotic discs (Bio-Rad, Marnes-la Coquette, France) were used for control. Discs were placed onto the surface of the agar plates previously smeared with the indicator cultures. Plates were incubated at 30 °C for 24 h and followed the diameter of the inhibition zones (in mm) were recorded. Assay was performed in duplicate. In addition, an assay to determine the Minimal Inhibitory Concentration (MIC) of the compound able to inhibit growth of the four indicators was carried out. 96-well plates were used with each well containing different volumes (140 – 180 µL) of TSB or BHI broth, 20 µL of an overnight culture of *S. aureus* CECT 86, *L. monocytogenes* CECT 4031, *E. coli* CECT 99 or *K. pneumoniae* CECT 143T and different volumes (0 – 40 µL) of the solution 5 mg/mL of (CH<sub>3</sub>)<sub>2</sub>NH<sub>2</sub>[Fe(phen)Cl<sub>4</sub>] in Milli-Q water to achieve concentrations of the compound in the well of between 0 µg/mL and 1000 µg/mL. The final volume in each well was 200 µL. To know initial cell population in the wells, a sample was taken of each of the wells and a viable cell count was carried out to know the growth of each of the indicators. Dilutions in sterile PBS pH = 7.2 were plated onto TSA or BHI agar plates, and plates incubated during 48 h at 37 °C. The plate was incubated during 22 h at 37 °C and absorbance at 630 nm (A<sub>630</sub>) was read every 30 min, previous a gentle stirring, using the reader Synergy HT (Biotek, USA). After 22 hours of incubation, a sample was taken of each of the wells and the procedure described above was carried out again to know the final cell population in the wells. Counts were expressed as colony forming units/mL and the percentage of growth obtained after 22 h of incubation with each concentration of the compound with respect to that of the indicator without compound was calculated. All the assays were performed in triplicate.



**Figure. S1** Solubility of the complex  $(\text{CH}_3)_2\text{NH}_2[\text{Fe}(\text{phen})\text{Cl}_4]$  in some selected solvents.

**Table S1:** Crystal data and structure refinement parameters of complex **1**.

$\text{C}_{14}\text{H}_{16}\text{Cl}_4\text{FeN}_3$	$\gamma = 104.883 (2)^\circ$
$M_r = 423.95 \text{ g/mol}$	$V = 881.61 (12) \text{ \AA}^3$
Triclinic, $P\bar{1}$	$Z = 2$
$a = 8.4271 (7) \text{ \AA}$	$F(000) = 430$
$b = 8.5571 (7) \text{ \AA}$	$D_x = 1.597 \text{ Mg m}^{-3}$
$c = 12.7653 (10) \text{ \AA}$	Mo $K\alpha$ radiation, $\lambda = 0.71073 \text{ \AA}$
$\alpha = 97.119 (3)^\circ$	$\mu = 1.46 \text{ mm}^{-1}$
$\beta = 91.008 (2)^\circ$	$T = 296 \text{ K}$
76536 measured reflections	$\theta_{\text{max}} = 39.4^\circ, \theta_{\text{min}} = 2.5^\circ$
10482 independent reflections	$h = -15 \rightarrow 15$
8526 reflections with $I > 2\sigma(I)$	$k = -15 \rightarrow 15$
$R_{\text{int}} = 0.036$	$l = -22 \rightarrow 22$
Refinement on $F^2$	0 restraints
Least-squares matrix: full	Hydrogen site location: inferred from neighbouring sites
$R[F^2 > 2\sigma(F^2)] = 0.027$	H-atom parameters constrained
$wR(F^2) = 0.079$	$w = 1/[\sigma^2(F_o^2) + (0.0399P)^2 + 0.1124P]$ where $P = (F_o^2 + 2F_c^2)/3$
$S = 1.04$	$(\Delta/\sigma)_{\text{max}} = 0.002$
10482 reflections	$\Delta\rho_{\text{max}} = 0.46 \text{ e \AA}^{-3}$
201 parameters	$\Delta\rho_{\text{min}} = -0.53 \text{ e \AA}^{-3}$

**Table S2:** Fractional atomic coordinates and isotropic or equivalent isotropic displacement parameters ( $^{\circ}\text{A}^2$ ).

	x	y	z	$U_{\text{iso}}^*/U_{\text{eq}}$
Fe1	0.82531 (2)	0.72071 (2)	0.22208 (2)	0.02568 (3)
Cl1	0.99611 (3)	0.53092 (3)	0.18387 (2)	0.03481 (4)
Cl2	0.64811 (3)	0.87646 (3)	0.27829 (2)	0.03861 (5)
Cl3	0.74486 (3)	0.67653 (3)	0.04407 (2)	0.03787 (5)
Cl4	1.05095 (3)	0.93969 (3)	0.21612 (2)	0.03612 (5)
N1	0.88309 (9)	0.70229 (8)	0.38677 (5)	0.02688 (11)
N2	0.64103 (9)	0.50527 (9)	0.25757 (5)	0.02846 (12)
N3	0.81548 (11)	0.25627 (11)	-0.00688 (7)	0.03954 (17)
H3A	0.8940	0.2609	-0.0530	0.047*
H3B	0.8371	0.3527	0.0334	0.047*
C1	1.00104 (12)	0.80442 (11)	0.45056 (7)	0.03342 (16)
H1	1.0706	0.8917	0.4237	0.040*
C2	1.02485 (14)	0.78598 (13)	0.55669 (8)	0.0401 (2)
H2	1.1077	0.8608	0.5994	0.048*
C3	0.92516 (15)	0.65699 (14)	0.59700 (7)	0.0412 (2)
H3	0.9388	0.6441	0.6676	0.049*
C4	0.80136 (12)	0.54344 (12)	0.53079 (7)	0.03356 (16)
C5	0.78482 (10)	0.57303 (10)	0.42596 (6)	0.02655 (12)
C6	0.65781 (10)	0.46539 (10)	0.35573 (6)	0.02717 (12)
C7	0.55439 (12)	0.32720 (11)	0.39120 (8)	0.03494 (17)
C8	0.57633 (15)	0.29859 (14)	0.49804 (9)	0.0445 (2)
H8	0.5088	0.2070	0.5217	0.053*
C9	0.69335 (16)	0.40233 (15)	0.56489 (8)	0.0442 (2)
H9	0.7041	0.3819	0.6342	0.053*
C10	0.42945 (13)	0.22826 (13)	0.31934 (10)	0.0447 (2)
H10	0.3606	0.1335	0.3383	0.054*
C11	0.40996 (13)	0.27245 (13)	0.22135 (10)	0.0455 (2)
H11	0.3256	0.2099	0.1741	0.055*

C12	0.51832 (12)	0.41268 (12)	0.19294 (8)	0.03684 (18)
H12	0.5038	0.4420	0.1264	0.044*
C13	0.65778 (17)	0.2303 (2)	-0.06565 (14)	0.0626 (4)
H13A	0.6356	0.1294	-0.1124	0.094*
H13B	0.6627	0.3186	-0.1062	0.094*
H13C	0.5718	0.2259	-0.0169	0.094*
C14	0.8238 (3)	0.1325 (2)	0.06018 (15)	0.0750 (5)
H14A	0.7463	0.1327	0.1144	0.112*
H14B	0.9327	0.1559	0.0922	0.112*
H14C	0.7979	0.0272	0.0182	0.112*

**Table S3:** Bond distances (Å) and bond angles (°) of the complex **1**.

Fe1—N1	2.1835 (7)	C1—C2	1.4002 (13)
Fe1—N2	2.1856 (7)	C2—C3	1.3669 (17)
Fe1—Cl4	2.3114 (3)	C3—C4	1.4112 (15)
Fe1—Cl2	2.3117 (3)	C4—C5	1.4035 (11)
Fe1—Cl3	2.3167 (3)	C4—C9	1.4338 (15)
Fe1—Cl1	2.4447 (3)	C5—C6	1.4328 (11)
N1—C1	1.3281 (10)	C6—C7	1.4071 (11)
N1—C5	1.3567 (10)	C7—C10	1.4080 (16)
N2—C12	1.3285 (11)	C7—C8	1.4323 (15)
N2—C6	1.3532 (10)	C8—C9	1.3497 (19)
N3—C14	1.4562 (18)	C10—C11	1.3699 (18)
N3—C13	1.4663 (17)	C11—C12	1.4007 (13)
N1—Fe1—N2	75.47 (3)	C14—N3—C13	115.26 (13)
N1—Fe1—Cl4	92.79 (2)	N1—C1—C2	122.63 (9)
N2—Fe1—Cl4	167.59 (2)	C3—C2—C1	119.39 (9)
N1—Fe1—Cl2	89.31 (2)	C2—C3—C4	119.57 (8)
N2—Fe1—Cl2	88.50 (2)	C5—C4—C3	117.10 (9)



Cl4—Fe1—Cl2	95.467 (12)	C5—C4—C9	119.13 (9)
N1—Fe1—Cl3	167.02 (2)	C3—C4—C9	123.77 (9)
N2—Fe1—Cl3	93.47 (2)	N1—C5—C4	123.00 (8)
Cl4—Fe1—Cl3	97.672 (10)	N1—C5—C6	117.16 (7)
Cl2—Fe1—Cl3	97.267 (11)	C4—C5—C6	119.83 (8)
N1—Fe1—Cl1	84.01 (2)	N2—C6—C7	122.93 (8)
N2—Fe1—Cl1	84.34 (2)	N2—C6—C5	117.32 (7)
Cl4—Fe1—Cl1	90.533 (12)	C7—C6—C5	119.73 (8)
Cl2—Fe1—Cl1	171.237 (10)	C6—C7—C10	117.07 (9)
Cl3—Fe1—Cl1	88.228 (10)	C6—C7—C8	119.11 (9)
C1—N1—C5	118.28 (7)	C10—C7—C8	123.77 (9)
C1—N1—Fe1	126.71 (6)	C9—C8—C7	121.08 (9)
C5—N1—Fe1	115.00 (5)	C8—C9—C4	121.07 (9)
C12—N2—C6	118.53 (7)	C11—C10—C7	119.60 (8)
C12—N2—Fe1	126.54 (6)	C10—C11—C12	119.38 (10)
C6—N2—Fe1	114.93 (5)	N2—C12—C11	122.42 (9)
C5—N1—C1—C2	-1.64 (13)	C4—C5—C6—N2	176.02 (7)
Fe1—N1—C1—C2	177.45 (7)	N1—C5—C6—C7	178.58 (7)
N1—C1—C2—C3	0.96 (15)	C4—C5—C6—C7	-2.39 (12)
C1—C2—C3—C4	0.81 (15)	N2—C6—C7—C10	0.21 (14)
C2—C3—C4—C5	-1.75 (14)	C5—C6—C7—C10	178.53 (9)
C2—C3—C4—C9	178.48 (9)	N2—C6—C7—C8	-177.11 (9)
C1—N1—C5—C4	0.58 (12)	C5—C6—C7—C8	1.20 (13)
Fe1—N1—C5—C4	-178.62 (6)	C6—C7—C8—C9	0.46 (16)
C1—N1—C5—C6	179.57 (8)	C10—C7—C8—C9	-176.67 (11)
Fe1—N1—C5—C6	0.38 (9)	C7—C8—C9—C4	-0.95 (17)
C3—C4—C5—N1	1.10 (12)	C5—C4—C9—C8	-0.25 (15)
C9—C4—C5—N1	-179.12 (8)	C3—C4—C9—C8	179.51 (10)
C3—C4—C5—C6	-177.87 (8)	C6—C7—C10—C11	-2.34 (16)

C9—C4—C5—C6	1.91 (12)	C8—C7—C10—C11	174.85 (11)
C12—N2—C6—C7	2.15 (13)	C7—C10—C11—C12	2.12 (18)
Fe1—N2—C6—C7	-177.57 (7)	C6—N2—C12—C11	-2.43 (15)
C12—N2—C6—C5	-176.20 (8)	Fe1—N2—C12—C11	177.26 (8)
Fe1—N2—C6—C5	4.08 (9)	C10—C11—C12—N2	0.31 (18)
N1—C5—C6—N2	-3.01 (11)		

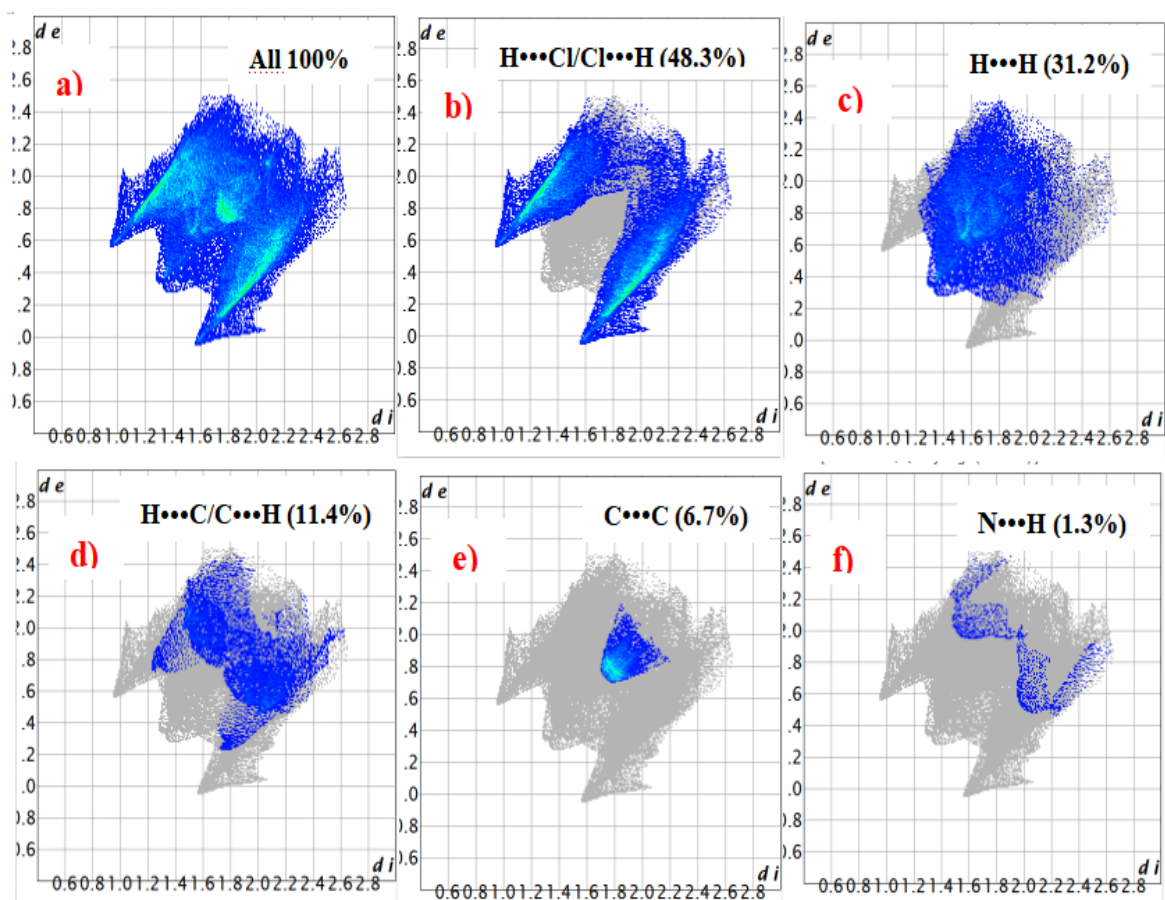


**Figure. S2** The 2D fingerprint plots of the major contacts of  $(\text{CH}_3)_2\text{NH}_2[\text{Fe}(\text{phen})\text{Cl}_4]$ , showing contributions from different contacts: b)  $\text{H}\cdots\text{Cl}/\text{Cl}\cdots\text{H}$ , c)  $\text{H}\cdots\text{H}$ , d)  $\text{H}\cdots\text{C}/\text{C}\cdots\text{H}$ , e)  $\text{C}\cdots\text{C}$  and f)  $\text{N}\cdots\text{H}/\text{H}\cdots\text{N}$ .

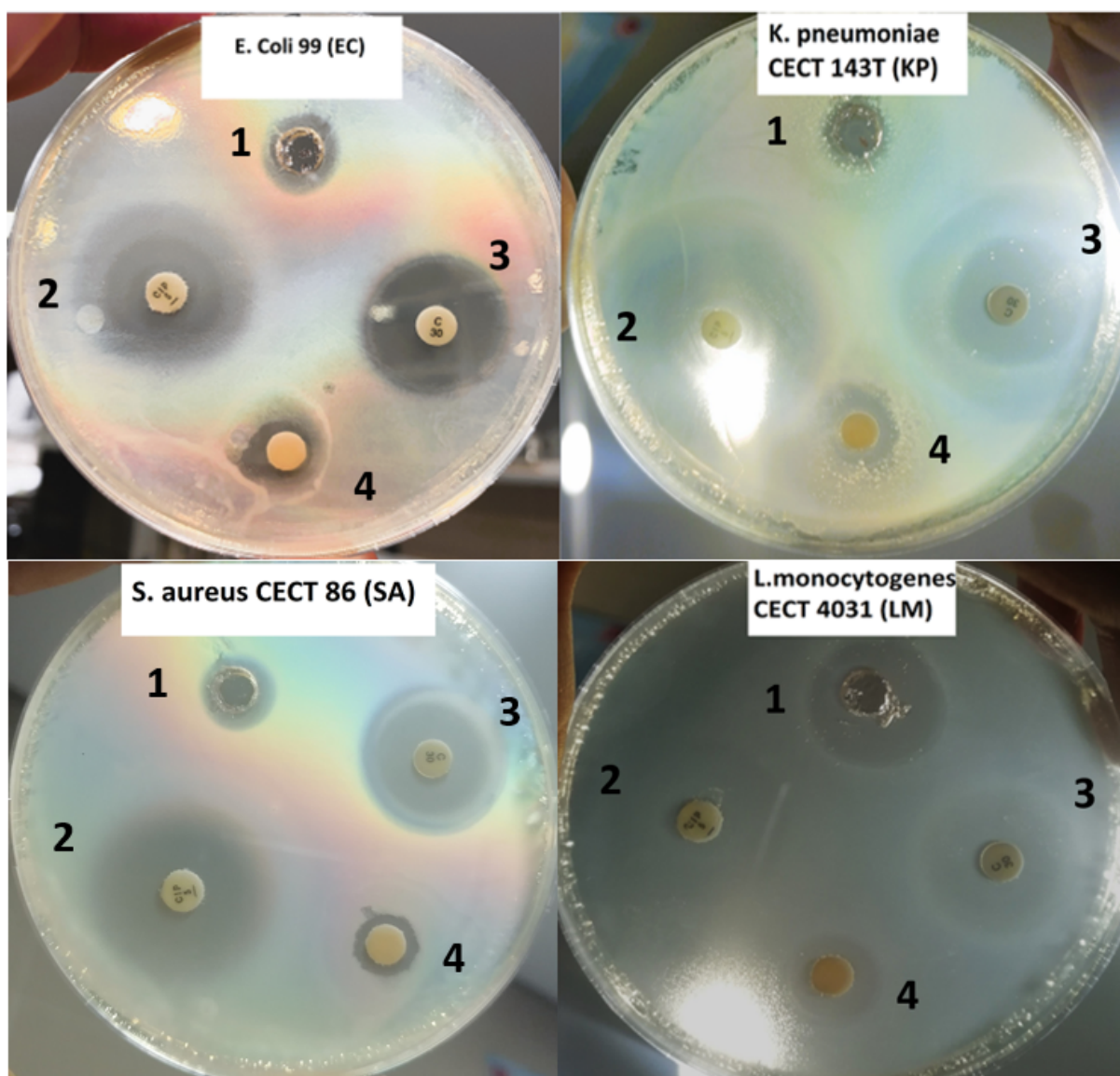


**Figure. S3** Inhibition zone of  $(\text{CH}_3)_2\text{NH}_2[\text{Fe}(\text{phen})\text{Cl}_4]$  and the commercially available antibiotic in (mm) at 600  $\mu\text{g}/\text{mL}$  concentration. 1 and 4 are Blank discs spotted with 20  $\mu\text{L}$  of a 5 mg/mL of compound 1, while 2 is Ciprofloxacin (5  $\mu\text{g}$ ) antibiotic disc and 3 is chloramphenicol (30  $\mu\text{g}$ ) antibiotic one.

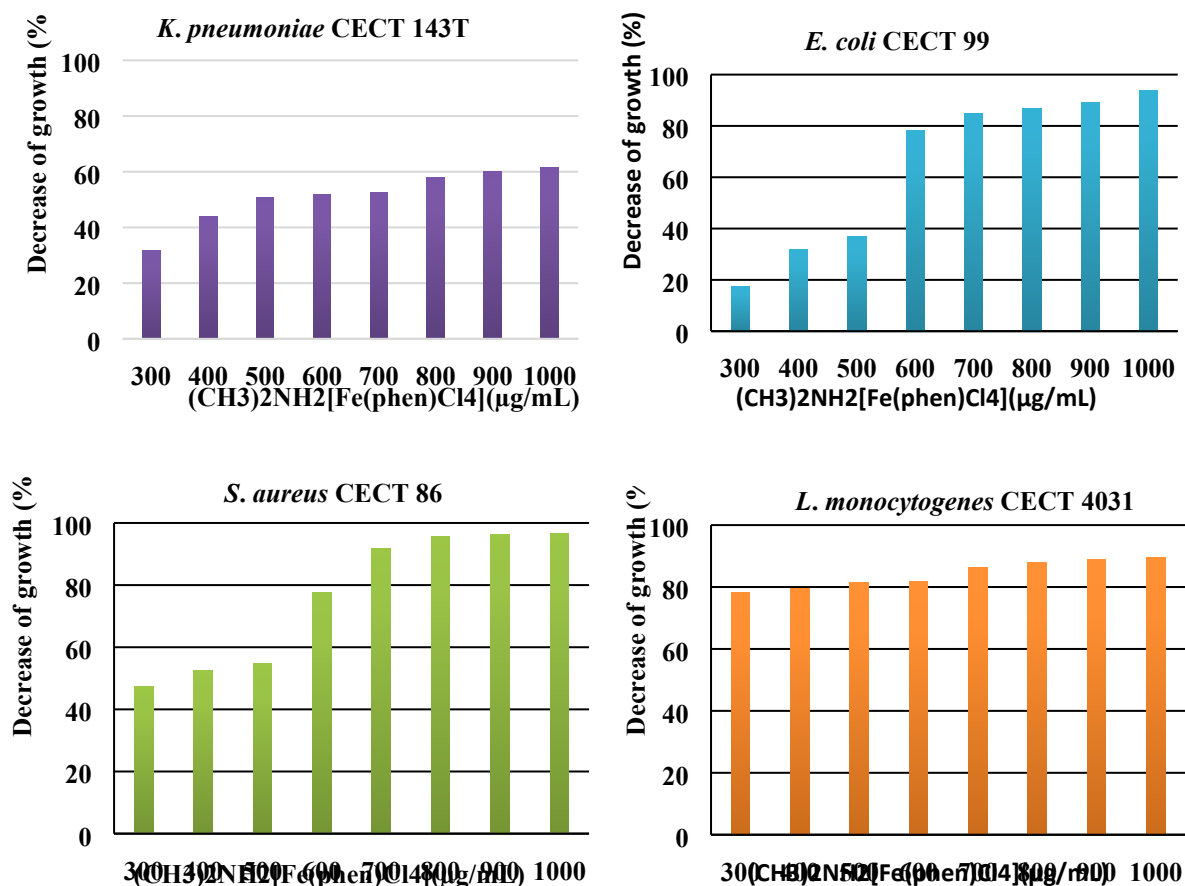


**Figure. S4** In vitro antimicrobial activity of  $(\text{CH}_3)_2\text{NH}_2[\text{Fe}(\text{phen})\text{Cl}_4]$  against two Gram-negative and two Gram-positive bacteria.

## References

1. G. M. Sheldrick, *Acta Crystallogr. A.*, 2008, **64**, 112-122.
2. G. M. Sheldrick, *Acta Crystallogr. A: Found. Adv.*, 2015, **71**, 3-8.
3. M. A. Spackman and J. J. McKinnon, *CrystEngComm.*, 2002, **4**, 378-392.
4. P. Spackman, M. Turner, J. McKinnon, S. Wolff, D. Grimwood, D. Jayatilaka and M. Spackman, *J. Appl. Crystallogr.*, 2021, **54**.
5. H. P. Fleming, J. L. Etchells and R. N. Costilow, *Appl Microbiol.*, 1975, **30**, 1040-1042.